NANO LETTERS

Letter

Cite This: Nano Lett. 2019, 19, 5774−5780

pubs.acs.org/NanoLett

Assembling Ordered Crystals with Disperse Building Blocks

Peter J. Santos,[†] Tung Chun Cheung,[†] and Robert J. Macfarlane*

Department of Materials Science and Engineering, Massachusetts Institute of Technology, 77 Massachusetts Avenue, Cambridge, Massachusetts 02139, United States

Supporting Information

ABSTRACT: Conventional colloidal crystallization techniques typically require low dispersity building blocks in order to make ordered particle arrays, resulting in a practical challenge for studying or scaling these materials. Nanoparticles covered in a polymer brush therefore may be predicted to be challenging building blocks in the formation of high-quality particle superlattices, as both the nanoparticle core and polymer brush are independent sources of dispersity in the system. However, when supramolecular bonding between complementary functional groups at the ends of the polymer chains are used to drive particle assembly, these "nanocomposite tectons" can make high quality superlattices with polymer dispersities as large as 1.44 and particle diameter relative standard deviations up to 23% without any significant change to superlattice crystallinity. Here we demonstrate and explain how the flexible and dynamic nature of the polymer chains that comprise the particle brush allows them to deform to accommodate the irregularities in building block size and shape that arise from the inherent dispersity of their constituent components. Incorporating "soft" components into nanomaterials design therefore offers a facile and robust method for maintaining good control over organization when the materials themselves are imperfect.

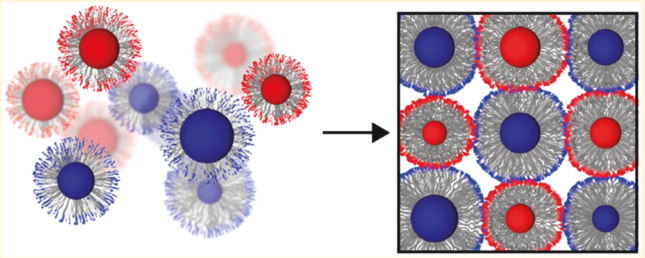

KEYWORDS: *Nanoparticles, self-assembly, dispersity, polymer brushes, supramolecular chemistry*

Colloidal crystallization is an effective means of manipulating material structure at the nanometer length scale, as chemical interactions between nanoparticle building blocks can be used to program their assembly into ordered lattices.[1,2] A wide variety of surface ligands have been used to control these interactions and thereby manipulate particle assembly, where the most stable phases typically maximize either particle packing density or the number of favorable interactions between particles' surface ligands.[3,4] In all of these strategies, particle size and shape dispersity are regarded as a negative factor that must be overcome to create well-ordered crystals, as irregularity in building block shape results in inefficient packing and limitations to interparticle surface contacts.[5−7] As a result, many impressive strategies to minimize dispersity in the particle assembly process have been developed, including multiple techniques for the synthesis of monodisperse particles of different shapes,[8−10] the use of biopolymer cages to dictate the directionality of interparticle bond formation,[11,12] or even the use of molecularly precise biomacromolecules with controlled surface functionalization as colloidal building blocks.[13−15] However, all of these methods have limits in the composition of the particles that can be used and tend to result in a trade-off between the quality and quantity of the building blocks that can be made.

In contrast to colloidal crystallization approaches that aim to use the least disperse building blocks possible, we have recently reported a new self-assembling particle called the Nanocomposite Tecton (NCT), which uses inherently nonuniform synthetic polymers as surface ligands (Figure 1).[16] Interestingly, although NCTs have dispersity originating from both their nanoparticle core and their polymer brush, they can still form lattices with long-range order. We hypothesize that the ability of NCTs to spontaneously form crystalline lattices despite their inherent size and shape inhomogeneity arises from the ability of the polymer brush to easily deform as a means of maximizing favorable supramolecular interactions between particles. Thus, the establishment of appropriate design and processing strategies could enable these "soft" building blocks to overcome significant variations in either particle core size or ligand length.[17−19] Here we explain how the concept of ligand softness affects the processing pathways used to obtain NCT-based colloidal crystals, as well as how these highly deformable surface ligands can mask imperfections in particle size or shape during assembly.[20] Ultimately, this strategy allows for highly disperse nanoparticle components (up to 23% variation in particle core diameter) to form superlattice architectures without any reduction in crystal quality, well beyond the ∼2−10% limit that is typically required for maximizing the quality of other colloidal crystals. As a result, NCTs represent a unique building block for nanomaterial synthesis that has significant potential for making scalable particle-based materials.

Received: June 20, 2019
Revised: July 25, 2019
Published: July 26, 2019

DOI: 10.1021/acs.nanolett.9b02508
Nano Lett. 2019, 19, 5774−5780

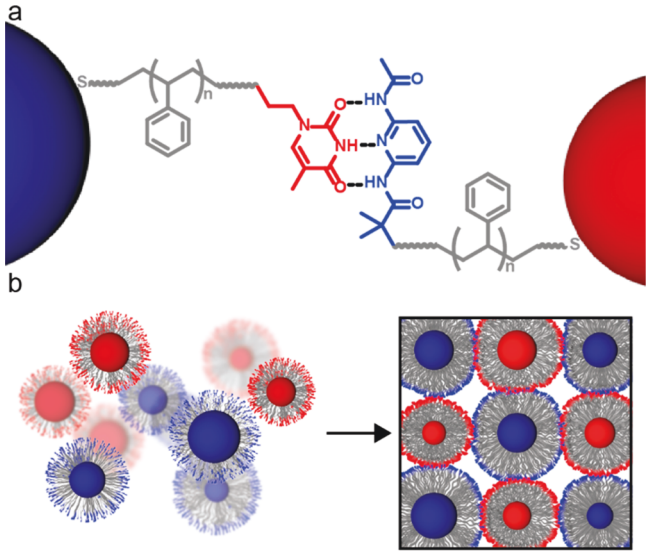

Figure 1. Nanocomposite Tecton assembly scheme. (a) NCTs consist of a nanoparticle core, a polymer shell, and a supramolecular binding group. When complementary NCTs are combined, hydrogen bonds form between them to drive assembly. (b) Particles containing a soft, polymeric shell are more tolerant of dispersity, and when coupled with an enthalpic driving force they can crystallize into well-organized structures.

The NCTs used in this work consist of gold nanoparticle (AuNP) cores coated with polystyrene brushes (Figure S1) that terminate in either diaminopyridine (DAP) or thymine (Thy) motifs that constitute a complementary hydrogen bonding pair. When NCTs with complementary supramolecular binding groups are combined, multiple hydrogen bonds form between the particles; these bonding interactions have been demonstrated to drive the formation of body-centered cubic (bcc)-type superlattices when the NCTs are thermally annealed.[16] NCTs are amenable to thermal annealing because the hydrogen bonding interactions are relatively weak, and heating to mild temperatures (below 80 °C) is therefore sufficient to enable rearrangement. Given the inherent dispersity in both the particle sizes and shapes (previous work has demonstrated crystals for particle sizes with a relative standard deviation (RSD) of 15% and polymers with $Đ$ of ∼1.1), the ability of NCTs to adopt conformations with long-range order is somewhat surprising. Understanding and controlling how these soft, high dispersity polymer shells affect crystallization therefore requires first determining how crystal formation is affected by processing pathway, as well as any upper bound in crystal quality that may be imposed on these assembled lattices via the use of a nonuniform and deformable polymer ligand coating.

The simplest potential thermal annealing profile to generate ordered NCT arrays is to heat and hold the initially amorphous aggregates at a temperature close to their melting temperature (T_m),[21] analogous to recrystallization and grain growth processes in classical atomic systems (Figure 2a).[22] When this thermal annealing profile is used, the NCTs are able to form an ordered lattice but small-angle X-ray scattering (SAXS) data indicate that this annealing profile results in highly polycrystalline samples with small grain sizes ∼250 nm in diameter. The small average size of these grains is not entirely unexpected, as the dispersity of the polymer brush

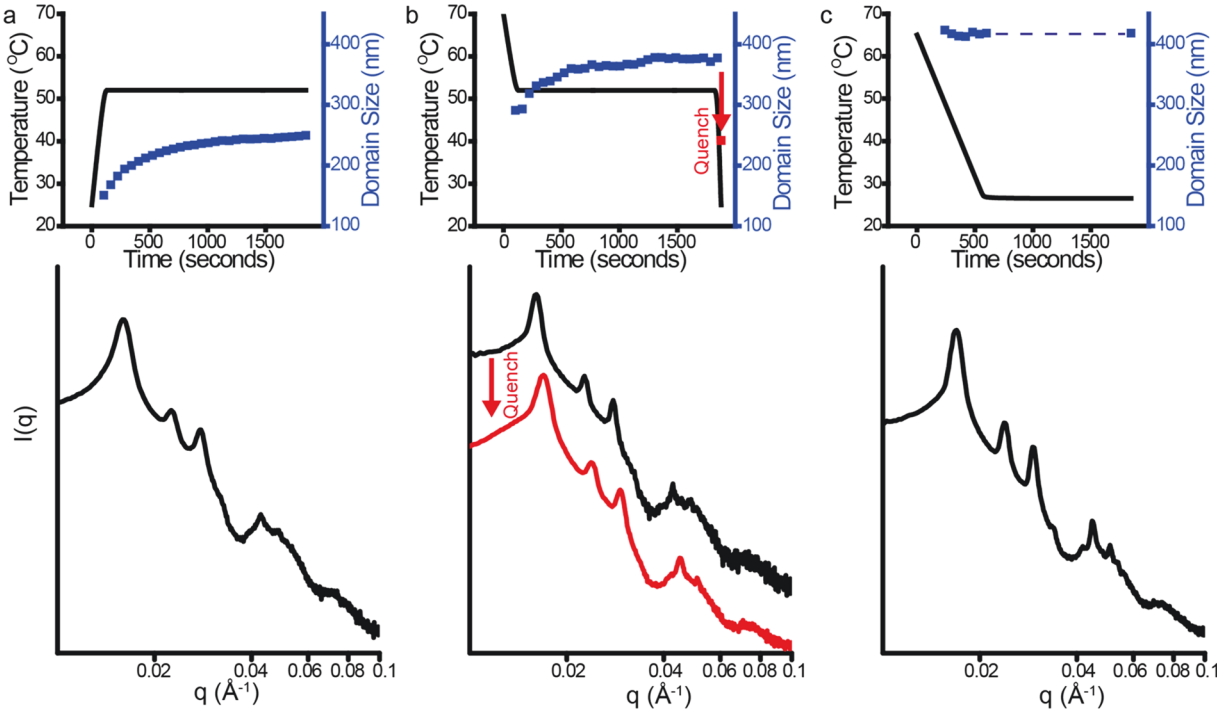

Figure 2. In situ SAXS measurements of NCT crystallization. (a) Temperature profile of NCTs heated from room temperature to their T_m and held there while they crystallize (black trace). Annealing results in a gradual increase in domain size, as estimated by the Scherrer equation, but after a 30 min treatment the crystal quality is still poor (blue data points). (b) When NCTs are cooled from an elevated temperature, the nucleation and growth process results in larger crystalline domains. However, further quenching from T_m to room temperature causes the formation of additional amorphous phase aggregates from unassembled NCTs. (c) Cooling the NCTs from an elevated temperature at 4 °C/min results in highly ordered crystals at all temperatures.

DOI: 10.1021/acs.nanolett.9b02508
Nano Lett. 2019, 19, 5774−5780

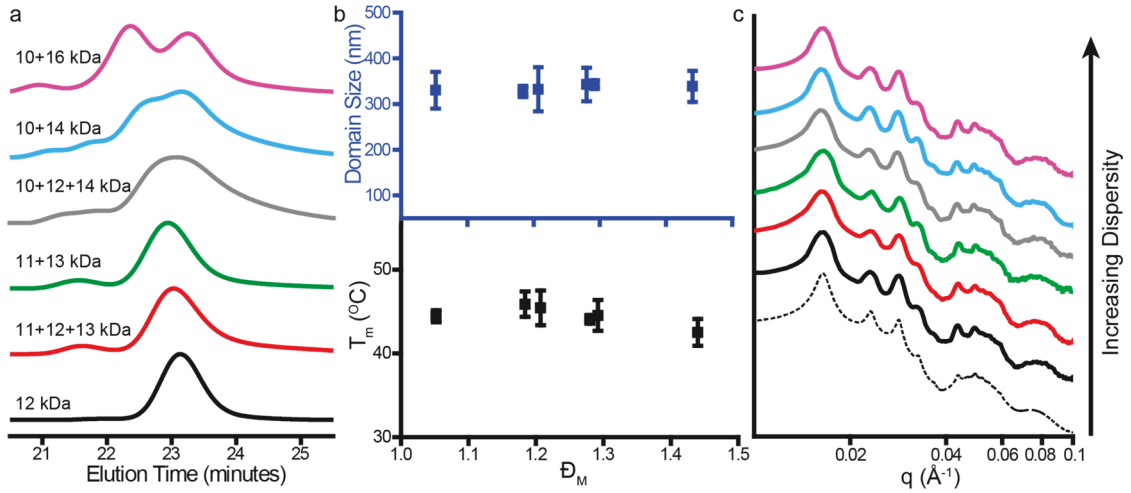

Figure 3. NCT assembly is not strongly affected by the dispersity of the polymer shell. (a) GPC traces showing the increasingly disperse batches of polymers used in NCT synthesis. All polymer batches have a number-average molecular weight of 12 kDa, polymer dispersity is controlled by blending together multiple low dispersity polymers of different molecular weights. (b) The melting temperature of the NCTs (bottom), indicative of the strength of NCT−NCT association, does not have a strong relationship with polymer dispersity. Additionally, there is no statistically significant difference in domain size, as estimated by the Scherrer equation (top) for NCTs assembled with polymers of varying dispersity. Error bars represent standard deviations, $n = 3$. (c) SAXS diffraction patterns of NCTs assembled with increasingly disperse polymers. The dashed line is a simulated SAXS diffraction pattern of a bcc crystal structure.

heights and the flexibility of the polymer chains means that the number of DAP-Thy complexes that can form in a perfectly ordered state and a kinetically trapped state should be similar. Because the driving force for assembling NCTs is the formation of supramolecular complexes, the energy difference between these two states with similar numbers of hydrogen bonds would be predicted to be relatively small, reducing the thermodynamic force for forming large crystallites.

To avoid the formation of the kinetic traps that limit crystal grain size, an alternate annealing pathway would be to heat the NCTs until completely melted, then drop the solution to just below the T_m and hold the NCTs in this state until crystal formation is complete (Figure 2b). This thermal profile should grow large, high quality crystals because quenching the sample just below its melting temperature suppresses the number of nucleation events, resulting in a small number of initial crystallites that grow to form large grains. Indeed, this formation pathway is commonly used to generate large atomic or molecular crystals.[23] However, although the initial aggregates that formed immediately below T_m were more crystalline than the samples heated from room temperature, quenching from this high T (to 25 °C) resulted in a noticeable reduction in crystal quality (as indicated by the broader peaks in the SAXS pattern). This reduction in quality stems from the fact that NCTs exist in equilibrium between their assembled and melted state across a large thermal window; this broad melting transition arises from the multivalent nature of the bonding interactions between particles (Figure S5).[24,25] Therefore, to give the largest domains, the NCT solution must be brought into equilibrium at each temperature between the fully melted and fully aggregated states. Interestingly, when the NCTs are slowly cooled across this thermal window, the resulting crystals exhibit a sharper SAXS diffraction pattern corresponding to larger grain sizes (~400 nm) but these crystal sizes reach a maximum early in the transition and only become more numerous instead of larger (Figure S7a). This upper limit on domain size is likely due to the fact that crystallites of a given mass can be observed to precipitate out of solution; whereas some small amounts of additional growth may occur due to individual NCTs attaching to these precipitated structures, grain growth rates are limited compared to the solution-suspended aggregates. Therefore, at temperatures within the thermal window between the fully aggregated and fully melted state there exists an equilibrium between free NCTs dispersed in solution and precipitated aggregates that are unlikely to either grow or reorganize, indicating that the crystallite sizes observed in Figure 2c represent a practical maximum. This limitation in domain size was confirmed by controlling the rate of cooling during NCT crystallization. For cooling rates slower than 8 °C/s, only a slight increase in crystal quality or domain size was observed as the cooling rate was decreased (Figure S7). Nevertheless, the kinetic traps caused by both the dispersity in NCT size and the soft nature of their bonding interactions can be minimized by using a solution cooling rate to control the nucleation and growth rates of crystals in solution within this fundamental limit.

Given that NCT crystallization arises from the formation of multiple DAP and Thy hydrogen bonds, it therefore could be hypothesized that altering the dispersity of the polymer brush height could also affect crystallization by altering the ability of DAP and Thy groups on adjacent particles to form supramolecular complexes. Larger variations in polymer chain lengths across the surface of an NCT would be expected to decrease crystallinity, as they would effectively alter the overall shape of each NCT, and therefore the thermodynamic driving forces for forming ordered arrays. To investigate the effects of polymer dispersity on NCT crystallization, a series of DAP-terminated polymers ranging in molecular weight from 10 to 16 kDa, each with $Đ < 1.05$, was synthesized by atom transfer radical polymerization (ATRP).[26] $Đ$ of the NCT polymer brushes was varied by combining these batches of low-dispersity polymers in different ratios to obtain polymer blends where the average polymer length remained constant at ~12 kDa, but the overall values of $Đ$ varied between 1.05 and 1.44 (a value that might be obtained from an uncontrolled free radical polymerization).[27] We would note that control

DOI: 10.1021/acs.nanolett.9b02508
Nano Lett. 2019, 19, 5774−5780

experiments were also performed to ensure that the polymer grafts on the NCTs possessed the same polymer length distributions as the polymer stocks used to functionalize each batch of particles. In other words, the values of $Đ$ for the polymer brushes on each NCT were identical to the values of $Đ$ of the stock solutions (Figure S2). These samples were then annealed by slowly cooling them from high temperatures to obtain the most ordered lattice possible.

Surprisingly, no correlation between polymer dispersity and crystallinity was observed; all of the samples exhibited indistinguishable SAXS patterns, indicating that the final crystal structures were identical in quality. Even NCTs with a strongly bimodal distribution of polymer lengths showed no change in their average crystallite domain size, lattice parameter, or degree of long-range ordering (Figure 3b,c).

Prior theoretical work[28] has described polymer brushes containing chains with varying molecular weight and can provide an interpretation consistent with the experimental results presented here. Specifically, the preservation of crystallinity suggests the NCTs retain an isotropic configuration, even when loaded with disperse polymer brushes. Prior models and experiments suggest that having high and low molecular weight polymers adjacent to one another is energetically favorable due to a positive entropy of mixing, and therefore no phase segregation or patches of different polymer lengths are expected to occur along the surface of the particle, although there may be differences in the brush conformation.[28−30] More simply, although individual polymer chains lengths can vary, the average brush height remains largely isotropic across the surface of the entire particle.

Nevertheless, individual polymer chains may experience different entropic penalties when confined within an NCT−NCT bond. When adjacent NCTs form DAP-Thy hydrogen bonds, the polymer chains engaged in bonding experience a severe reduction in the number of accessible conformations, resulting in a large decrease in entropy. When an NCT brush consists of polymer chains of varying molecular weight, the magnitude of this change in entropy would be dependent on polymer length, as shorter polymer chains whose ends are not already near the surface of the NCT require additional conformation restriction in order to form hydrogen bonds (i.e., shorter chains need to stretch more to reach their NCT neighbors).

It is therefore surprising that increasing the dispersity of the polymer brush does not affect the binding strength of the NCTs, as indicated by their relatively static T_m regardless of polymer dispersity (Figure 3b). However, the prior model mentioned above suggests that a polymer brush can minimize its free energy by segregating the chain ends along the brush height coordinate of the system as a function of polymer molecular weight.[28] In other words, it is energetically unfavorable for the longer polymers to bury their chain ends in the interior of the brush, but instead they will on average have their termini further from the surface of the particle than the shorter ones. As a result, interactions between the longest polymer chains on bound NCTs would dominate the thermodynamics of NCT assembly, explaining the lack of significant variation in either crystal quality or melting temperature as a function of brush dispersity.

To further verify this hypothesis, NCTs were coloaded with a bimodal mixture of varying fractions of long and short polymer chains. NCTs made with the two different polymers have a stark difference in T_m, (~10 °C difference between the 10 and 16 kDa NCTs), meaning that monitoring the T_m of NCTs consisting of mixtures of these polymer lengths could potentially indicate which polymer length dictates the strength of inter-NCT bonding (Figure S6). Interestingly, doping a low molecular weight polymer brush with longer chains has different effects on NCT thermodynamics than doping a high molecular weight brush with shorter polymer chains (Figure 4a). When shorter polymers are doped into the long-

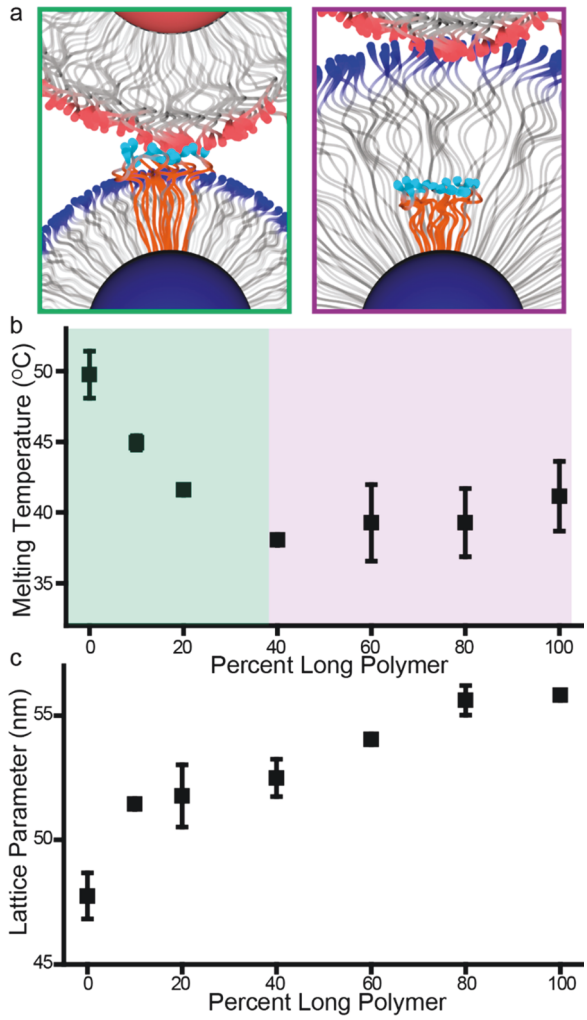

Figure 4. Assembling NCTs with bimodal mixtures of long and short polymer chains reveals the dynamics of the polymer brush. (a) Polymer chains that are significantly longer than the average brush height are presented at the periphery of the NCT and are thus always able to participate in bonding (left). Conversely, polymer chains that are significantly shorter than the average brush height are buried in the polymer brush and do not readily participate in interparticle bonding (right). (b) Increasing the fraction of long polymer chains in the bimodal distribution (mixtures of 10 and 16 kDa polymers) decreases the melting temperature of the NCTs. However, when the fraction of a long polymer surpasses 40%, the melting temperature plateaus at a value corresponding to the T_m of NCTs functionalized with just the long polymer. This trend suggests the assembly behavior is dominated by only the longer polymer chains. (c) Despite the lack of change in T_m above the 40% longer polymer, the interparticle spacing consistently increases with the growing fraction of long polymer, signifying the presence of the shorter polymers are still contributing to the overall height of the brush by altering the free volume occupied by the longer polymer chains.

DOI: 10.1021/acs.nanolett.9b02508
Nano Lett. 2019, 19, 5774−5780

polymer NCTs (right-most data points, Figure 4b), the T_m remains largely unchanged. This lack of change in T_m is consistent with the hypothesis that shorter chains dispersed among an otherwise high molecular weight brush would be forced to undergo significant stretching to reach the bonding plane between NCTs, and the corresponding entropy penalty associated with this stretching means that it is energetically unfavorable for them to strongly contribute to NCT assembly. Thus, the T_m remains fairly constant with an increasing amount of shorter polymers in a majority long-polymer brush.

Alternatively, when longer polymers are added to a low molecular weight brush, the melting temperature quickly drops (left-most data points, Figure 4b). The supramolecular binding groups on these longer chains are close to the exterior of the NCT, and can readily participate in hydrogen bonding, regardless of the length of the nearby polymer chains. As a result, the height of the brush gradually increases with increasing amounts of longer polymer, as is reflected in the larger lattice parameter (Figure 4c). The shorter polymers are forced to incur an entropic stretching penalty to participate in bonding, resulting in a lowered T_m. As the necessary degree of stretching increases with a larger fraction of longer polymer, hydrogen bonds between the shorter polymers no longer improve the stability of the lattice. Above this point (~40% long polymer for this system), these longer chains are able to dominate the assembly process, dictating the thermodynamics of NCT assembly (indicating the lack of substantial change in T_m between 40% and 100% long polymer). The observation that longer polymer chains can encapsulate the shorter ones in the brush are in agreement with prior experimental work.[31] Therefore, dispersity in polymer molecular weight has a minimal effect on the overall dimensions of the NCT, as the brush can stretch and compress to account for local variations in polymer length.

Although the softness of the polymer brush is observed to aid in NCT crystal formation despite any inherent inhomogeneity in polymer chain length, the nanoparticle core of NCTs is an additional source of dispersity in the NCT architecture, and unlike the polymer brush it is not capable of dynamically changing its shape. In colloidal crystals formed due to entropically driven close packing, small variations in particle size make the formation of ordered lattices impossible, even in the case of polymer grafted nanoparticles.[32,33] In hard-sphere packing, it has been theoretically calculated and experimentally shown that the order−disorder transition is thermodynamically prohibited above a terminal dispersity between 6 and 11%.[34,35] Prior work has demonstrated that adding bonding interactions that drive lattice formation via enthalpy maximization can enable more disperse building blocks to form ordered arrays. However, these systems still have limitations in the amount of dispersity that can be tolerated. For example, colloids coated with rigid dsDNA typically only form ordered arrays at particle dispersities of ~10% or less, and only when the length of the DNA ligands is comparable to the radius of the particles being assembled.[36] Other examples have also been demonstrated to create mesoscale structures from disperse mixtures of nanoparticles but these typically occur through fractionalization or self-limiting processes that do not incorporate all particles present in solution or do not control particle coordination environment.[37,38] Given the above-demonstrated ability of the NCT polymer brush to accommodate significant variations in polymer brush height, it could also be hypothesized that NCTs may be able to tolerate greater deviations in particle size or shape than these previous colloidal crystallization methods.

To confirm this prediction, NCTs were synthesized with nanoparticle core diameters of 19, 24, and 28 nm, each with a particle diameter relative standard deviation (RSD) < 11.5%. The three different sizes were combined in ratios that maintained an average diameter of 24 nm but varied the overall distribution of inorganic particle core sizes up to ~23% (representing a bimodal distribution of 19 and 28 nm spheres, Figure S3). These samples were annealed by slow cooling through their melting temperature and analyzed with SAXS. Astonishingly, all samples with the exception of the 23% RSD system exhibited crystals of identical quality, and even the 23% RSD sample exhibited only slight traces of a nonuniform crystal structure (evidenced by a slight shoulder in the SAXS pattern at $q \sim 0.011$) (Figure 5). There was also no observed shift in the average lattice parameter as a function of particle size dispersity, nor was there any evidence of observable phase segregation of the smaller or larger particles within a crystal. If the larger and smaller particles phase segregated into separate

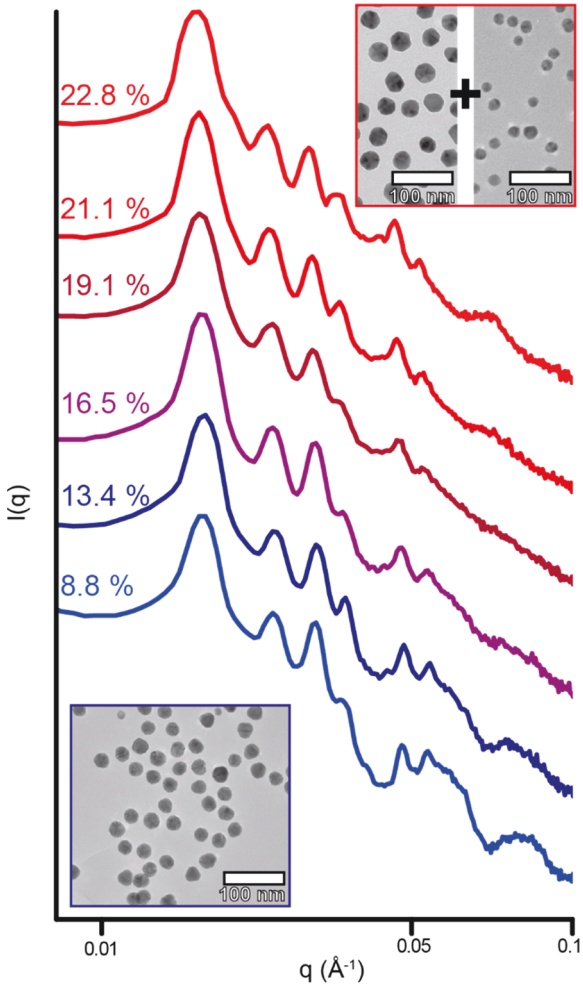

Figure 5. SAXS patterns of NCT assemblies synthesized with varying nanoparticle core dispersities. Combinations of 19, 24, and 28 nm AuNPs were used to prepare sets of NCTs where each NCT batch had an average core diameter of 24 nm but RSDs ranged from 8.8% to 22.8% (inset numbers). After thermal processing, all sets of NCTs were able to form bcc crystals with almost no discernible change to crystal quality.

DOI: 10.1021/acs.nanolett.9b02508
Nano Lett. 2019, 19, 5774−5780

crystallites, this would be noted by a gradual broadening of the SAXS peaks with increasing deviation in particle sizes, as well as a reduced number of observable higher order peaks due to this broadening. In other words, the final state would consist of multiple different crystallites with varying lattice parameters due to the differences in particle core diameters in each crystallite; this is clearly not observed in the SAXS patterns, which all exhibit nearly identical peak widths and number of higher order scattering peaks. Furthermore, the changes in the scattering patterns' form factors at higher q (~0.05−0.1) indicate that the dispersity of the particles within the lattices correlates with the dispersity of the NCT stock solutions (Figure S4).[39] Finally, the fact that all particles in each sample precipitated out of solution, combined with the observation that there was no difference in crystal quality or lattice parameter at different points within the precipitate also implies that the RSD in particle size within each lattice is comparable to the initial RSD of particle sizes in the stock solutions. In short, the softness of the polymer ligands appears to completely mask variations in particle size or shape within the regime studied, meaning that even at 23% RSD (mixtures of NCTs with 19 and 28 nm average core sizes), the soft polymer brushes adjusted to allow all particles to form an average crystal lattice parameter. The degree of deformation of the polymer brush required to assemble such disperse nanoparticles (~5 nm) is comparable to the amount of polymer stretching measured previously (Figure 4c), consistent with these prior results. It is hypothesized that shorter polymers would be less capable of deforming and so would only tolerate smaller variations in nanoparticle core size.

The surprising ability of NCTs to crystallize even with particle size deviations several times greater than is typically required by multiple other colloidal assembly methods can be understood by examining how NCT design differs from these more commonly studied nanoparticle superlattice building blocks. Colloidal crystals that assemble through a drying-mediated process require that each particle be as close to uniformity as possible, as these crystals do not have a deep energy minimum and thus variance in particle diameter can significantly reduce the favorability of packing. This trend can even be observed even when assembling polymer brush-coated particles that are soft and capable of deforming to accommodate deviations in particle size, as the lack of an enthalpic driving force means that alterations to packing fraction (and thus entropy) can have a significant destabilizing effect on assembly. However, because NCTs are assembled via supramolecular bonding, the enthalpic driving force for NCT crystallization is much stronger, offsetting some of the entropic considerations that are affected by particle dispersity. NCTs do get stuck in kinetic traps as a result of these enthalpic bonding interactions, but proper thermal processing is effective at overcoming them. Dispersity is therefore hypothesized to mostly affect NCTs through geometric obstruction, where differences in particle size cause such severe lattice strain that the formation of large crystalline domains becomes unlikely.

The ability to synthesize ordered nanomaterials from highly disperse building blocks solves a persistent problem in colloidal self-assembly, as producing uniform nanoparticles is often impractical at the relevant quantities required to synthesize bulk solids.[40] Additionally, the facile manipulation of the various structural features of NCTs allows them to provide insight into how particle crystallization occurs when "soft" bonds drive the assembly process. Moreover, NCTs are potentially amenable to the use of size- and shape-disperse nanoparticle building blocks that may not form ordered crystals when using other assembly methods.[33−35] NCTs are therefore a useful platform for understanding colloidal self-assembly, and their easy processing and resistance to dispersity make them a valid candidate for the scalable synthesis of ordered nanomaterials.

■ ASSOCIATED CONTENT

Supporting Information

The Supporting Information is available free of charge on the ACS Publications website at DOI: 10.1021/acs.nanolett.9b02508.

Materials and Methods; Scheme S1; Figures S1−S7; Tables S1−S5 Supplementary References 1−5 (PDF)

■ AUTHOR INFORMATION

Corresponding Author

*E-mail: rmacfarl@mit.edu.

ORCID

Robert J. Macfarlane: 0000-0001-9449-2680

Author Contributions

†P.J.S. and T.C.C. contributed equally.

Notes

The authors declare no competing financial interest.

■ ACKNOWLEDGMENTS

This work was primarily supported by an NSF CAREER Grant, award number CHE-1653289, and made use of the MRSEC Shared Experimental Facilities at MIT, supported by the NSF under Award DMR 14-19807. P.J.S. acknowledges support by the NSF Graduate Research Fellowship Program under Grant 1122374. SAXS experiments at beamline 12-ID-B at the Advanced Photon Source at Argonne National Laboratory were supported by the U.S. Department of Energy, Office of Science, Office of Basic Energy Sciences, under contract DE-AC02-06CH11357. This work benefited from the use of the SasView application, originally developed under NSF award DMR-0520547. SasView contains code developed with funding from the European Union's Horizon 2020 research and innovation program under the SINE2020 project, Grant Agreement 654000.

■ REFERENCES

(1) Pileni, M.-P. Self-Assembly of Inorganic Nanocrystals: Fabrication and Collective Intrinsic Properties. *Acc. Chem. Res.* **2007**, *40* (8), 685−693.

(2) von Freymann, G.; Kitaev, V.; Lotsch, B. V.; Ozin, G. A. Bottom-up Assembly of Photonic Crystals. *Chem. Soc. Rev.* **2013**, *42* (7), 2528−2554.

(3) Bishop, K. J. M.; Wilmer, C. E.; Soh, S.; Grzybowski, B. A. Nanoscale Forces and Their Uses in Self-Assembly. *Small* **2009**, *5* (14), 1600−1630.

(4) Elacqua, E.; Zheng, X.; Shillingford, C.; Liu, M.; Weck, M. Molecular Recognition in the Colloidal World. *Acc. Chem. Res.* **2017**, *50* (11), 2756−2766.

(5) O'Brien, M. N.; Jones, M. R.; Mirkin, C. A. The Nature and Implications of Uniformity in the Hierarchical Organization of Nanomaterials. *Proc. Natl. Acad. Sci. U. S. A.* **2016**, *113* (42), 11717−11725.

(6) Shevchenko, E. V.; Talapin, D. V.; Kotov, N. A.; O'Brien, S.; Murray, C. B. Structural Diversity in Binary Nanoparticle Superlattices. *Nature* **2006**, *439* (7072), 55−59.

DOI: 10.1021/acs.nanolett.9b02508
Nano Lett. 2019, 19, 5774−5780

(7) Kotov, N. A.; Meldrum, F. C.; Wu, C.; Fendler, J. H. Monoparticulate Layer and Langmuir-Blodgett-Type Multiparticulate Layers of Size-Quantized Cadmium Sulfide Clusters: A Colloid-Chemical Approach to Superlattice Construction. *J. Phys. Chem.* **1994**, *98* (11), 2735−2738.
(8) Zheng, N.; Fan, J.; Stucky, G. D. One-Step One-Phase Synthesis of Monodisperse Noble-Metallic Nanoparticles and Their Colloidal Crystals. *J. Am. Chem. Soc.* **2006**, *128* (20), 6550−6551.
(9) O'Brien, M. N.; Jones, M. R.; Brown, K. A.; Mirkin, C. A. Universal Noble Metal Nanoparticle Seeds Realized Through Iterative Reductive Growth and Oxidative Dissolution Reactions. *J. Am. Chem. Soc.* **2014**, *136* (21), 7603−7606.
(10) Tao, A.; Sinsermsuksakul, P.; Yang, P. Tunable Plasmonic Lattices of Silver Nanocrystals. *Nat. Nanotechnol.* **2007**, *2* (7), 435−440.
(11) Liu, W.; Tagawa, M.; Xin, H. L.; Wang, T.; Emamy, H.; Li, H.; Yager, K. G.; Starr, F. W.; Tkachenko, A. V.; Gang, O. Diamond Family of Nanoparticle Superlattices. *Science* **2016**, *351* (6273), 582−586.
(12) Lo, P. K.; Karam, P.; Aldaye, F. A.; McLaughlin, C. K.; Hamblin, G. D.; Cosa, G.; Sleiman, H. F. Loading and Selective Release of Cargo in DNA Nanotubes with Longitudinal Variation. *Nat. Chem.* **2010**, *2* (4), 319−328.
(13) McMillan, J. R.; Brodin, J. D.; Millan, J. A.; Lee, B.; Olvera de la Cruz, M.; Mirkin, C. A. Modulating Nanoparticle Superlattice Structure Using Proteins with Tunable Bond Distributions. *J. Am. Chem. Soc.* **2017**, *139* (5), 1754−1757.
(14) McMillan, R. A.; Paavola, C. D.; Howard, J.; Chan, S. L.; Zaluzec, N. J.; Trent, J. D. Ordered Nanoparticle Arrays Formed on Engineered Chaperonin Protein Templates. *Nat. Mater.* **2002**, *1* (4), 247.
(15) Medalsy, I.; Dgany, O.; Sowwan, M.; Cohen, H.; Yukashevska, A.; Wolf, S. G.; Wolf, A.; Koster, A.; Almog, O.; Marton, I.; et al. SP1 Protein-Based Nanostructures and Arrays. *Nano Lett.* **2008**, *8* (2), 473−477.
(16) Zhang, J.; Santos, P. J.; Gabrys, P. A.; Lee, S.; Liu, C.; Macfarlane, R. J. Self-Assembling Nanocomposite Tectons. *J. Am. Chem. Soc.* **2016**, *138* (50), 16228−16231.
(17) Lynd, N. A.; Meuler, A. J.; Hillmyer, M. A. Polydispersity and Block Copolymer Self-Assembly. *Prog. Polym. Sci.* **2008**, *33* (9), 875−893.
(18) Si, K. J.; Chen, Y.; Shi, Q.; Cheng, W. Nanoparticle Superlattices: The Roles of Soft Ligands. *Adv. Sci.* **2018**, *5* (1), 1700179.
(19) Ye, X.; Zhu, C.; Ercius, P.; Raja, S. N.; He, B.; Jones, M. R.; Hauwiller, M. R.; Liu, Y.; Xu, T.; Alivisatos, A. P. Structural Diversity in Binary Superlattices Self-Assembled from Polymer-Grafted Nanocrystals. *Nat. Commun.* **2015**, *6*, 10052.
(20) Jishkariani, D.; Elbert, K. C.; Wu, Y.; Lee, J. D.; Hermes, M.; Wang, D.; van Blaaderen, A.; Murray, C. B. Nanocrystal Core Size and Shape Substitutional Doping and Underlying Crystalline Order in Nanocrystal Superlattices. *ACS Nano* **2019**, *13* (5), 5712−5719.
(21) Macfarlane, R. J.; Thaner, R. V.; Brown, K. A.; Zhang, J.; Lee, B.; Nguyen, S. T.; Mirkin, C. A. Importance of the DNA "Bond" in Programmable Nanoparticle Crystallization. *Proc. Natl. Acad. Sci. U. S. A.* **2014**, *111* (42), 14995−15000.
(22) Humphreys, F. J. A Unified Theory of Recovery, Recrystallization and Grain Growth, Based on the Stability and Growth of Cellular Microstructures—I. The Basic Model. *Acta Mater.* **1997**, *45* (10), 4231−4240.
(23) Brown, R. A. Theory of Transport Processes in Single Crystal Growth from the Melt. *AIChE J.* **1988**, *34* (6), 881−911.
(24) Jin, R.; Wu, G.; Li, Z.; Mirkin, C. A.; Schatz, G. C. What Controls the Melting Properties of DNA-Linked Gold Nanoparticle Assemblies? *J. Am. Chem. Soc.* **2003**, *125* (6), 1643−1654.
(25) Auyeung, E.; Li, T. I. N. G.; Senesi, A. J.; Schmucker, A. L.; Pals, B. C.; de la Cruz, M. O.; Mirkin, C. A. DNA-Mediated Nanoparticle Crystallization into Wulff Polyhedra. *Nature* **2014**, *505* (7481), 73−77.
(26) Matyjaszewski, K.; Xia, J. Atom Transfer Radical Polymerization. *Chem. Rev.* **2001**, *101* (9), 2921−2990.
(27) Fukuda, T.; Ma, Y. D.; Inagaki, H. Free-Radical Copolymerization. 3. Determination of Rate Constants of Propagation and Termination for Styrene/Methyl Methacrylate System. A Critical Test of Terminal-Model Kinetics. *Macromolecules* **1985**, *18* (1), 17−26.
(28) Milner, S. T.; Witten, T. A.; Cates, M. E. Effects of Polydispersity in the End-Grafted Polymer Brush. *Macromolecules* **1989**, *22* (2), 853−861.
(29) Bentz, K. C.; Savin, D. A. Chain Dispersity Effects on Brush Properties of Surface-Grafted Polycaprolactone-Modified Silica Nanoparticles: Unique Scaling Behavior in the Concentrated Polymer Brush Regime. *Macromolecules* **2017**, *50* (14), 5565−5573.
(30) Dodd, P. M.; Jayaraman, A. Monte Carlo Simulations of Polydisperse Polymers Grafted on Spherical Surfaces. *J. Polym. Sci., Part B: Polym. Phys.* **2012**, *50* (10), 694−705.
(31) Jiang, X.; Zhao, B.; Zhong, G.; Jin, N.; Horton, J. M.; Zhu, L.; Hafner, R. S.; Lodge, T. P. Microphase Separation of High Grafting Density Asymmetric Mixed Homopolymer Brushes on Silica Particles. *Macromolecules* **2010**, *43* (19), 8209−8217.
(32) Phillips, C. L.; Glotzer, S. C. Effect of Nanoparticle Polydispersity on the Self-Assembly of Polymer Tethered Nanospheres. *J. Chem. Phys.* **2012**, *137* (10), 104901.
(33) Choi, J.; Hui, C. M.; Schmitt, M.; Pietrasik, J.; Margel, S.; Matyjazsewski, K.; Bockstaller, M. R. Effect of Polymer-Graft Modification on the Order Formation in Particle Assembly Structures. *Langmuir* **2013**, *29* (21), 6452−6459.
(34) Bolhuis, P. G.; Kofke, D. A. Monte Carlo Study of Freezing of Polydisperse Hard Spheres. *Phys. Rev. E: Stat. Phys., Plasmas, Fluids, Relat. Interdiscip. Top.* **1996**, *54* (1), 634−643.
(35) Pusey, P. N. The Effect of Polydispersity on the Crystallization of Hard Spherical Colloids. *J. Phys. (Paris)* **1987**, *48* (5), 709−712.
(36) Park, S. Y.; Lytton-Jean, A. K. R.; Lee, B.; Weigand, S.; Schatz, G. C.; Mirkin, C. A. DNA-Programmable Nanoparticle Crystallization. *Nature* **2008**, *451* (7178), 553−556.
(37) Kalsin, A. M.; Fialkowski, M.; Paszewski, M.; Smoukov, S. K.; Bishop, K. J. M.; Grzybowski, B. A. Electrostatic Self-Assembly of Binary Nanoparticle Crystals with a Diamond-Like Lattice. *Science* **2006**, *312* (5772), 420−424.
(38) Xia, Y.; Nguyen, T. D.; Yang, M.; Lee, B.; Santos, A.; Podsiadlo, P.; Tang, Z.; Glotzer, S. C.; Kotov, N. A. Self-Assembly of Self-Limiting Monodisperse Supraparticles from Polydisperse Nanoparticles. *Nat. Nanotechnol.* **2011**, *6* (9), 580−587.
(39) Thünemann, A. F.; Rolf, S.; Knappe, P.; Weidner, S. In Situ Analysis of a Bimodal Size Distribution of Superparamagnetic Nanoparticles. *Anal. Chem.* **2009**, *81* (1), 296−301.
(40) Hatton, B.; Mishchenko, L.; Davis, S.; Sandhage, K. H.; Aizenberg, J. Assembly of Large-Area, Highly Ordered, Crack-Free Inverse Opal Films. *Proc. Natl. Acad. Sci. U. S. A.* **2010**, *107* (23), 10354−10359.

DOI: 10.1021/acs.nanolett.9b02508
Nano Lett. 2019, 19, 5774−5780